HOSTED BY

ELSEVIER

Available online at www.sciencedirect.com

ScienceDirect

journal homepage: www.elsevier.com/locate/jtte

Original Research Paper

Influence of shock absorber condition on pavement fatigue using relative damage concept

Pablo Kubo [a,*], *Cassio Paiva* [a], *Adelino Ferreira* [b], *Arthur Larocca* [c]

[a] *Department of Civil Engineering, State University of Campinas, Campinas, Brazil*
[b] *Department of Civil Engineering, University of Coimbra, Coimbra, Portugal*
[c] *Department of Engineering, Alpha Serviços de Assessoria Técnica Ltda, Curitiba, Brazil*

ARTICLE INFO

Article history:
Available online 9 October 2015

Keywords:
Vertical load
Pavement
Relative damage
Shock absorber

ABSTRACT

Considering the importance of the road transportation nowadays, concerns related to pavement deterioration and maintenance have become relevant subjects. Especially for commercial vehicles, the vertical dynamic load (characterized by the tire-road interaction) is directly related to wear on the road surface. Given this, the main objective of this paper is to analyse effects of vertical loads applied on the flexible pavement, considering the variation of the condition of shock absorbers from a truck's front suspension. The measurements were performed on a rigid truck, with 2 steering front axles, in a durability test track located in Brazil. With a constant load of 6 tons on the front suspension (the maximum allowed load on front axles according to Brazilian legislation), 3 different shock absorber conditions were evaluated: new, used and failed. By applying the relative damage concept, it is possible to conclude that the variation of the shock absorber conditions will significantly affect the vertical load applied on the pavement. Although the results clearly point to a dependent relationship between the load and the condition of the shock absorbers, it is recommended to repeat the same methodology, in future to analyse the influence of other quarter car model variants (such as spring rate, mass and tire spring stiffness).

1. Introduction

Besides the direct impact on the vehicle dynamic behaviour (rolling resistance, ride & handling, fuel economy, NVH), the tire-road interaction is also a factor that compromises the pavement integrity. As larger loads and vehicles appear in the road transportation system, pavement damage concerns become an increasingly relevant issue in road construction and maintenance activities (Fabela-Gallegos et al., 2010; Oliveira et al., 2008).

Vertical dynamic load is directly related to the deterioration of the pavement (Sayers et al., 1986). Therefore, this

* *Corresponding author*. Tel.: +55 41 91145783.
E-mail address: pyykubo@hotmail.com (P. Kubo).
Peer review under responsibility of Periodical Offices of Chang'an University.
http://dx.doi.org/10.1016/j.jtte.2015.10.001

relation can also be extended to vehicles variants, especially for commercial vehicles (trucks and buses). However, not all vehicles could cause equivalent damage because of the differences in wheel loads, number and location of axles, types of suspensions and tires, and other aspects (Gillespie et al., 1991).

By analysing a quarter car model (Fig. 1), it was expected that the shock absorber damping forces could be influenced by the natural wear of this system.

In Fig. 1, M_1 is sprung mass, Z is displacement of the sprung mass, K_1 is primary suspension spring rate, C_1 is shock absorber damping force, m_1 is unsprung mass, Z_u is displacement of the unsprung mass, K_1' is tire spring stiffness, Z_r is displacement of the ground.

The equations of motion for the quarter car model in Fig. 1 are shown as below (Simms and Crolla, 2002).

$$m_1\ddot{Z}_u = K_1'(Z_r - Z_u) - K_1(Z_u - Z) - C_1\left(\dot{Z}_u - \dot{Z}\right) \quad (1)$$

$$M_1\ddot{Z} = K_1'(Z_u - Z) + C_1\left(\dot{Z}_u - \dot{Z}\right) \quad (2)$$

Besides the fact that the damping forces (C_1) is a parameter of the quarter car model, it is not often considered in some studies regarding vertical load $m_1\ddot{Z}_u$ applied on the pavement (Che et al., 2011; Sun et al., 2011; Zhang and Zhang, 2011), or it is considered as a constant (Liu and Wang, 2008). In reality, the shock absorber damping forces varies in terms of compression and extension speed (Causemann and Kelchner, 2000).

The main objective of this paper is to analyse the influence of the shock absorber conditions on the vertical load damage on the pavement, using a simple instrumentation (metal-foil strain gauges) and the concept of relative damage.

2. Methodology

2.1. *Metal-foil strain gauge*

The metal-foil strain gauges (Fig. 2) are sensors made up of a thin resistive foil, fixed on an electrical insulation material called base (Andolfato et al., 2004) or matrix (Hannah and Reed, 1992). The main advantages and characteristics of the metal-foil strain gauges are their high precision and linearity, low cost and good dynamic and static response (Lima et al., 2008).

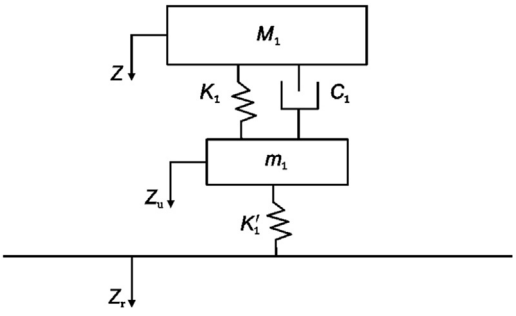

Fig. 1 – Quarter car model (Gillespie, 1992).

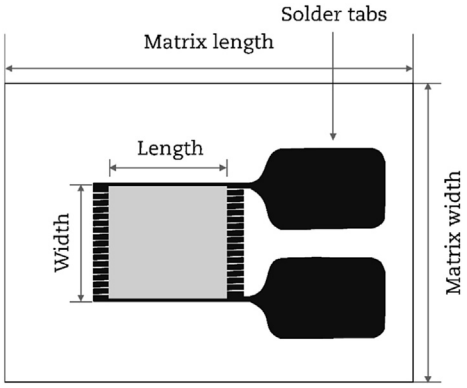

Fig. 2 – Illustration of a metal-foil strain gauge (Hannah and Reed, 1992).

The working principle of this gauge is based on the fact that all electrical conductors change their resistance when elongated (Gallina, 2003). This characteristic is stated in the Second Ohm's Law, which relates the resistance (R) of a conductor to its length (L), cross-sectional area (A) and resistivity (ρ).

$$R = \frac{\rho L}{A} \quad (3)$$

Considering a generic elongation in an electrical conductor, Eq. (3) can be rewritten as follow

$$\frac{\Delta R}{R} = \frac{k\Delta L}{L} \quad (4)$$

where the factor k is defined as the sensitivity of the strain gauge, corresponding to a constant that varies with the resistive material used (Andolfato et al., 2004; Gallina, 2003). Considering that the giving strain is measured as the total elongation per unit length of the material, the following equation is obtained.

$$\frac{\Delta R}{R} = k\epsilon \quad (5)$$

The Eq. (5) indicates that the magnitude of the measured strain (ϵ) is proportional to a relative change of resistance, which is the working principle of this type of sensor (Andolfato et al., 2004; Doebelin, 1990).

2.2. *Damage calculation*

As structures and mechanical components are regularly subjected to oscillating loads and fatigue is one of the major causes in component failures, fatigue life prediction has become a relevant subject (Liou et al., 1999). If a test specimen is subjected to a sufficiently severe cyclic stress, a fatigue crack or other damage will develop, resulting in the complete failure of the component/system (Dowling, 2012).

Through a stress-life (Wöhler) curve, as shown in Fig. 3, it is possible to estimate the number of cycles for component to failure on a determined magnitude of cycle stress. Unfortunately, only a few applications present such behaviour (regular and sinusoidal stress loads).

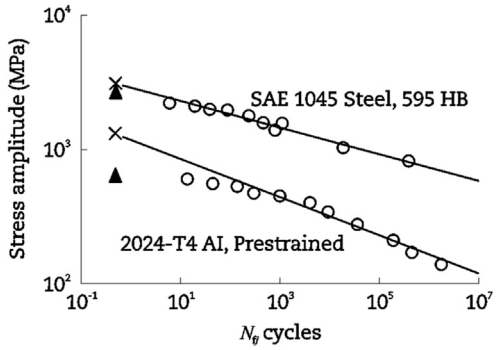

Fig. 3 – Example of 2 stress-life curves (Dowling, 2004).

Within this scenario, Palmgren suggested the following equation

$$\frac{N_1}{N_{f1}}+\frac{N_2}{N_{f2}}+\frac{N_3}{N_{f3}}+\cdots=\sum\frac{N_j}{N_{fj}}=1 \tag{6}$$

where N_j is number of cycles for each constant load, N_{fj} is number of cycles (failure) from stress-life curve for each constant load.

Basically, Palmgren states that a component will fail when the sum of the ratio of the number of cycles for each segment to the number of cycles from stress-life curves is equal to 1. Moreover, the damage, represented by those ratios, occurs and accumulates only when the stress is higher than the fatigue limit (Zhu et al., 2011).

On the other hand, Dowling highlights that for loads with high variation levels, it is not feasible to do the calculation as stated by Palmgren–Miner (Miner, 1945). In this way, it is necessary to adopt a procedure called rainflow cycle counting, created by Matsushi and Endo (1968). This analysis considers a cycle counting, which follows the criteria shown in Fig. 4.

With the combination of the peak-valley-peak "A-B-C" (Fig. 4), it will be considered as a cycle, if the amplitude variation $\Delta\sigma_{BC}$ is equal to or greater than the previous amplitude variation (Matsushi and Endo, 1968).

Finally, using the concepts from Palmgren–Miner/Endo and Matsushi, it is possible to define the following equation for the absolute damage $\left(\sum\frac{N_j}{N_{fj}}\right)$.

$$\sigma_a=\frac{\sigma_{max}-\sigma_{min}}{2} \tag{7}$$

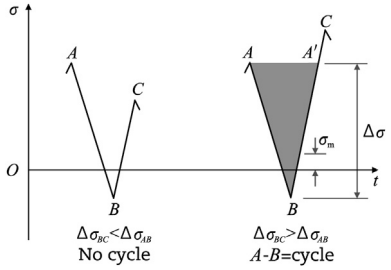

Fig. 4 – Rainflow cycle counting (Dowling, 2012).

Fig. 5 – Tested truck.

where σ_a is average amplitude from each rainflow cycle, σ_{max} is the maximum amplitude (peak) of each rainflow cycle, σ_{min} is the minimum amplitude (valley) of each rainflow cycle.

$$N_{fj}=\frac{1}{2}\left(\frac{\sqrt{\sigma_{max}\sigma_a}}{\sigma'_f}\right)^{\frac{1}{b}} \tag{8}$$

where σ'_f is theoretical loading that indicates failure with 0 cycle (material property), b is stress-life curve slope (material property).

2.3. *Boundaries and assumptions*

In order to analyse the influence of the shock absorber condition, it was necessary to keep the other variants of the quarter car model (Fig. 1) steady/fixed as follows.

(1) Sprung mass and unsprung mass were set as 6 tons, the maximum weight allowed on the front axle according to the Brazilian legislation;
(2) Primary suspension spring rate were set according to the manufacturing specification–new components;
(3) Tire pressure was set as 110 psi (7.6 bar);
(4) Pavement longitudinal profile tests were performed on a proving ground located in Brazil, in order to keep the same track in all measurements.

An 8 × 2 rigid truck was chosen (Fig. 5) and all measurements reflect the loads of both front steering axles.

2.4. *Instrumentation and calibration*

Uniaxial strain gauges were placed on the main leave spring of the 1st and 2nd steering axle (Fig. 6) on the left hand side (LHS) and right hand side (RHS) of the vehicle.

The recorded values given by the above-mentioned instrumentation were in με (micro-strain). Therefore, it was necessary to calibrate the system in order to estimate the force applied on the pavement.

A weighting scale was used and different loads were applied on the vehicle body with the objective of obtaining the calibration curves between με and the load applied on the ground in tons (Figs. 7 and 8).

Due to the fact that all tested springs have the same spring rate, all calibration curves have similar characteristics.

Fig. 6 – Primary suspension spring leaf-instrumentation.

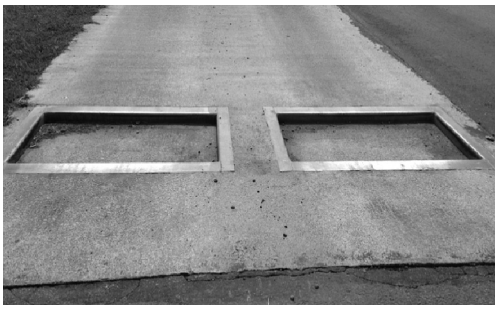

Fig. 9 – Detail of the pothole track.

Fig. 7 – Weighting scale used for calibration.

For the test procedure, a pothole (PH) track in the proving ground was used for the measurements with the following conditions (Figs. 9 and 10):

(1) Vehicle weight was 6 tons per front axle;
(2) Vehicle speed was 40 km/h;
(3) Tire pressure was 110 psi (7.6 bar) (ALAPA, 2013);
(4) Suspension spring used original primary suspension spring rate setting.

The only variant was the condition of the shock absorber: new, used (60,000 km of accumulated mileage) or failed (shock absorber with no damping force). The 3 measurements were performed for each test (as shock absorber condition). For the data analysis, all time signals were used.

3. Results and discussion

Fig. 11 presents an example of the time-series signal of each front spring for a shock absorber condition (new). The mentioned figure refers to the load applied to the pavement on each front axle tires, in tons.

Figs. 12–14 present the histograms for the tested shock absorber conditions. These diagrams can be visualized in a way that the counting cycles close to the static load (3 tons) are the mandatory values.

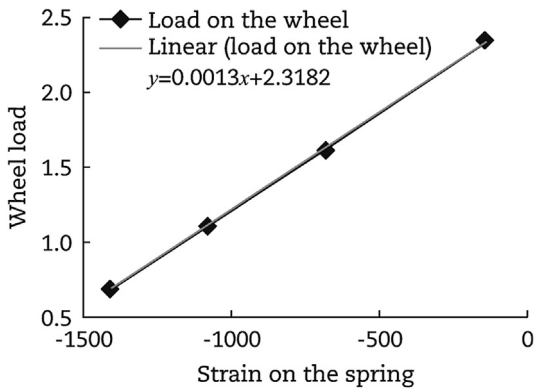

Fig. 8 – Example of one spring calibration (1st axle-LHS-front).

Fig. 10 – Interaction between tire and pothole.

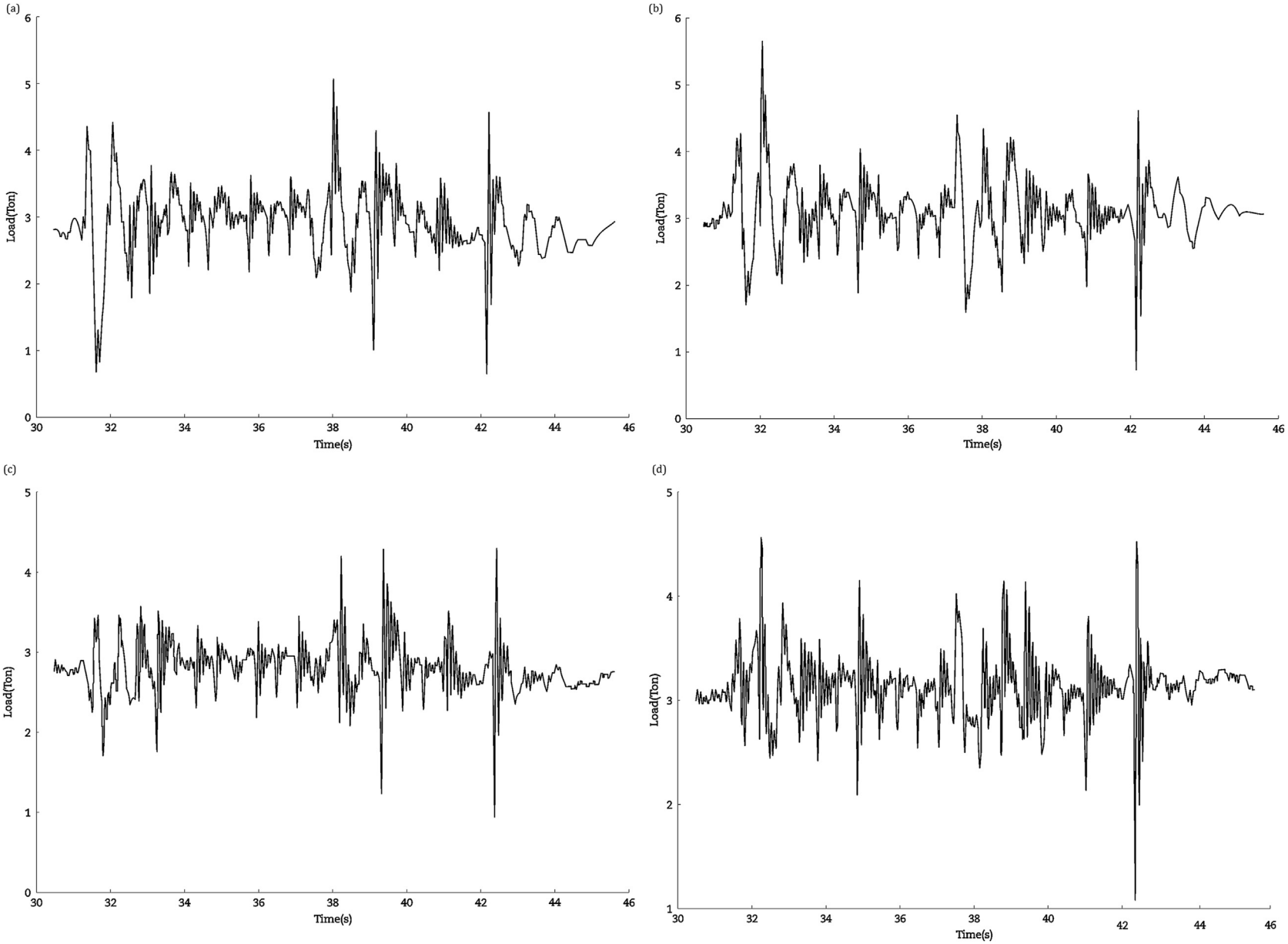

Fig. 11 – Time-series signal with new shock absorber on the pothole track. (a) 1st steering axle-LHS-load. (b) 1st steering axle-RHS-load. (c) 2nd steering axle-LHS-load. (d) 2nd steering axle-RHS-load.

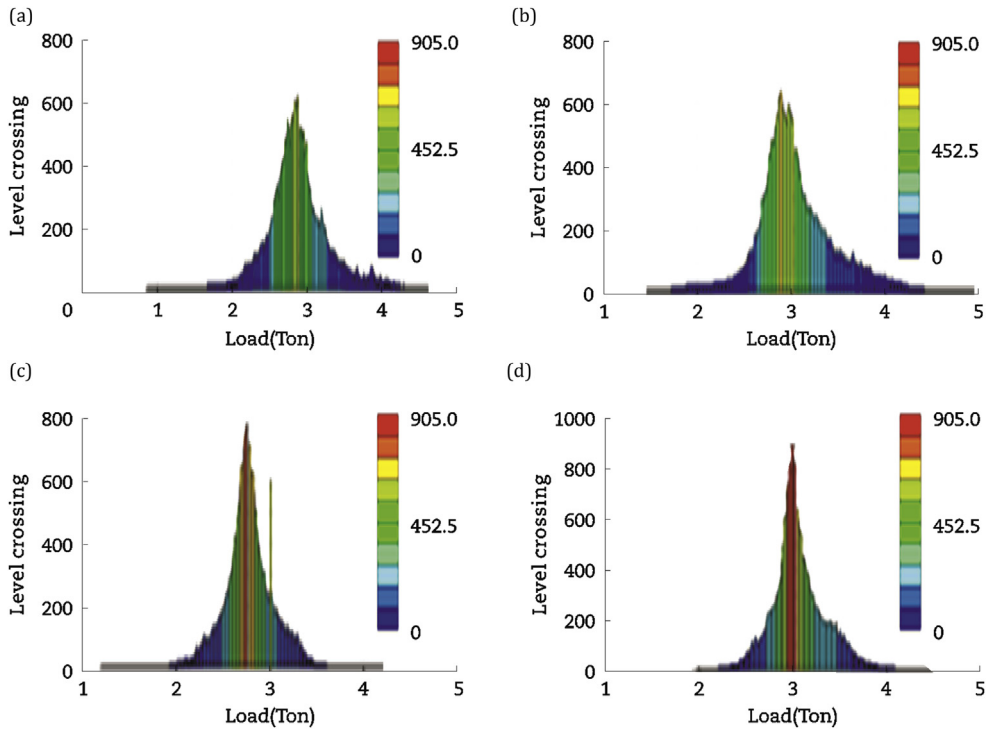

Fig. 12 – Level crossing histograms: new shock absorber. (a) 1st steering axle-LHS-load. (b) 1st steering axle-RHS-load. (c) 2nd steering axle-LHS-load. (d) 2nd steering axle-RHS-load.

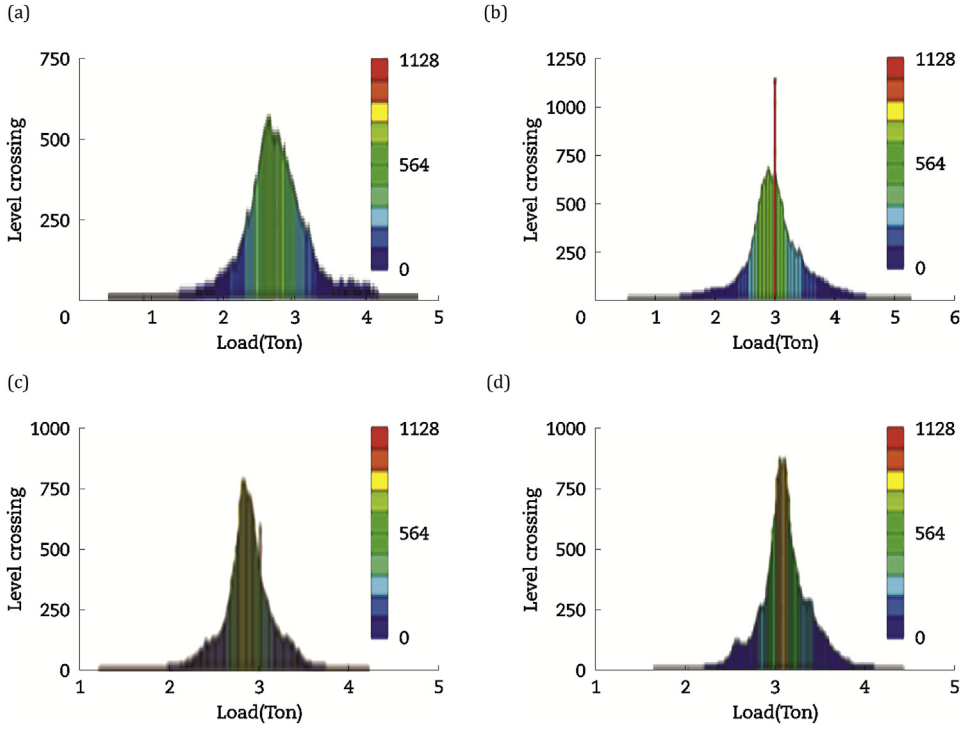

Fig. 13 – Level crossing histograms: used shock absorber. (a) 1st steering axle-LHS-load. (b) 1st steering axle-RHS-load. (c) 2nd steering axle-LHS-load. (d) 2nd steering axle-RHS-load.

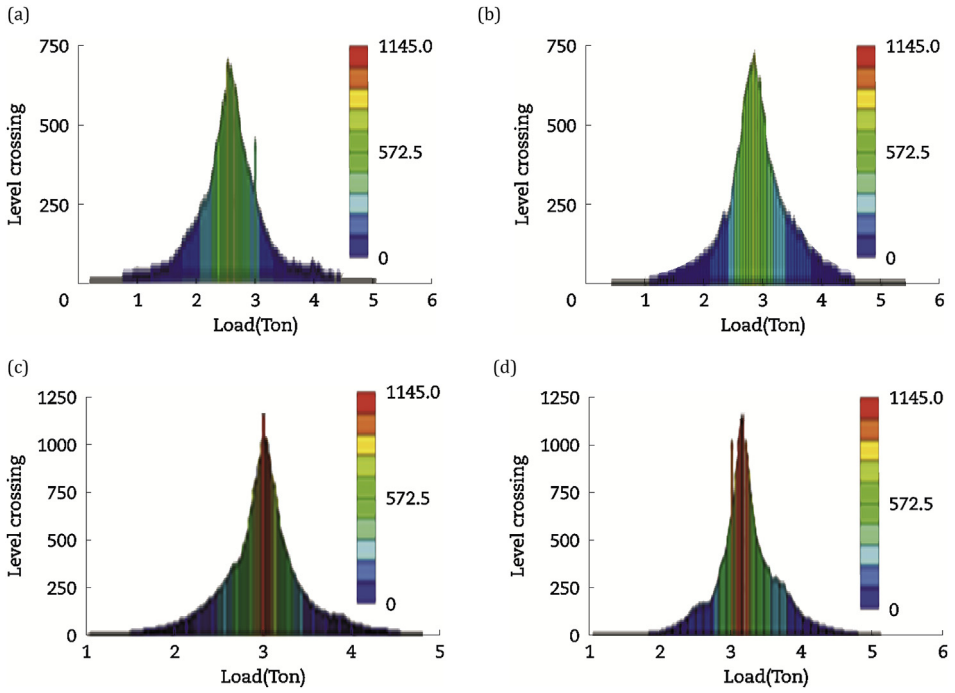

Fig. 14 – Level crossing histograms: failed shock absorber. (a) 1st steering axle-LHS-load. (b) 1st steering axle-RHS-load. (c) 2nd steering axle-LHS-load. (d) 2nd steering axle-RHS-load.

Nevertheless, with this statistical tool, it is not possible to precisely evaluate the influence of the shock absorber condition on pavement fatigue. Therefore, from the measured results and based on an artificial S–N curve, a relative damage analysis of the pavement was performed.

Fig. 15 presents the results for the relative damage on the pavement according to the shock absorber condition and for each front axle tires. The obtained results suggested that the shock absorber condition has a significant relation with the vertical load applied on the pavement and consequently to the relative damage on it. This analysis considered the new shock absorber condition as the baseline (fixed on 100%) and used a slope (k') of the S–N curve equal to 5.

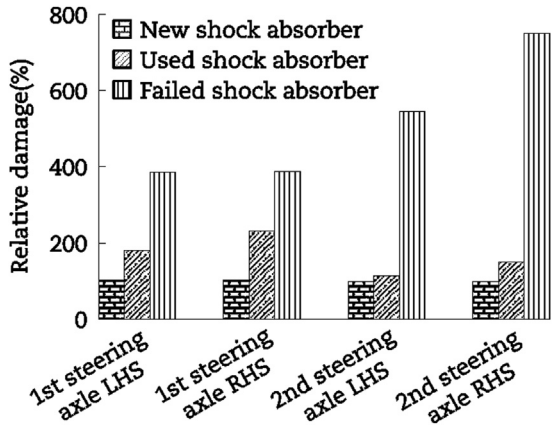

Fig. 15 – Relative damage among shock absorber conditions ($k' = 5$).

By analysing Fig. 15, it is noticeable that the first steering axle has a linear increment on pavement damage with the degradation of the shock absorber condition and that both sides (LHS and RHS) have the similar behaviour. On the other hand, this linearity is not observed on the 2nd steering axle, where the severity of the loading caused by this axle didn't increase up to the total failure of the damper. In addition, difference was found on the sides of the 2nd steering axle, which was higher on the RHS, due to the extra weight (fuel tank) on that area.

4. Conclusions

Three extreme shock absorber conditions have been analysed in order to identify their behaviour trends. However, it is important to highlight that the above-mentioned variation represents the entire lifetime of the component. Given this scenario, by applying the relative damage concept, it is possible to conclude that the variation of the shock absorber conditions will significantly affect the vertical load and consequently the damage made on the pavement.

For this first analysis, the other quarter car model variants, such as spring rate, tire pressure and spring mass were considered as constants, but it is recommended to apply the same methodology to those parameters, in order to have a complete view of the key factors that contribute to the increase of the pavement damage.

Finally, it is recommended to consider the real shock absorber damping forces, in order to identify any characteristics involving vehicle dynamics interaction with pavement.

REFERENCES

ALAPA, 2013. Tire Pressure Recommendation. ALAPA, São Paulo.

Andolfato, R.P., Camacho, J.S., Brito, G.A., 2004. Extensometria Básica. UNESP, Ilha Solteira.

Causemann, P., Kelchner, C., 2000. Automotive Shock Absorbers: Features, Designs, Applications, first ed. Verlag Moderne Industrie, Nünchen.

Che, F., Chen, S., Ma, Q., 2011. Change regularity by FEM for dynamic response of structural layers of asphalt pavement with dynamic load. In: 2011 International Conference on Multimedia Technology, Hangzhou, 2011.

Doebelin, E.O., 1990. Measurement System – Application and Design, fourth ed. McGraw-Hill, New York.

Dowling, N.E., 2004. Mean Stress Effects in Stress-life and Strain-life Fatigue. SAE Technical Paper 2004-01-2227. Society of Automotive Engineers. http://dx.doi.org/10.4271/2004-01-2227.

Dowling, N.E., 2012. Mechanical Behavior of Materials: Engineering Method for Deformation, Fracture and Fatigue, fourth ed. Prentice Hall, Upper Saddle River.

Fabela-Gallegos, M., Hernandez, R., Vazquez-Vega, D., et al., 2010. Evaluation of Contact Force and Pressure of Heavy Vehicle's Supersingle Tire versus Dual Tires. SAE Technical Paper 2010-01-1900. Society of Automotive Engineers. http://dx.doi.org/10.4271/2010-01-1900.

Gallina, R., 2003. Os extensômetros elétricos resistivos: evolução, aplicações e tendencies (Master thesis). Universidade São Judas Tadeu, São Paulo.

Gillespie, T.D., 1992. Fundamentals of Vehicle Dynamics. Society of Automotive Engineers, Warrandale.

Gillespie, T.D., Karamihas, S.M., Cebon, D., et al., 1991. Effects of Heavy Vehicle Characteristics on Pavement Response and Performance. University of Michigan, Ann Arbor.

Hannah, R.L., Reed, S.E., 1992. Strain Gage Users' Handbook. Chapman & Hall, London.

Lima, W., Rocha Neto, J., Lima, A., 2008. Measurement and control of deformation on a flexible beam using shape memory alloy. In: ABCM Symposium Series in Mechatronics, Campina Grande, 2008.

Liou, H.Y., Wu, W.F., Shin, C.S., 1999. A modified model for the estimation of fatigue life derived from random vibration theory. Probabilistic Engineering Mechanics 14 (3), 281–288.

Liu, L., Wang, Z., 2008. Influence of joints on ride quality and roughness index. Road Materials and Pavement Design 9 (1), 111–121.

Matsushi, M., Endo, T., 1968. Fatigue of Metals Subjected on Varying Stress. Japan Society of Mechanical Engineering, Fukouka.

Miner, M.A., 1945. Cumulative damage in fatigue. Journal of Applied Mechanics 12 (3), 156–164.

Oliveira, A., Valentim, C., Duarte, M., et al., 2008. Tire Pressure Impact on Structural Durability Tests Results. SAE Technical Paper 2008-36-0041. Society of Automotive Engineers. http://dx.doi.org/10.4271/2008-36-0041.

Sayers, M.W., Gillespie, T.D., Queiroz, A.V., 1986. The International Road Roughness Experiment: Establishing Correlation and a Calibration Standard for Measurements. HS-039 586. The World Bank, Washington DC.

Simms, A., Crolla, D., 2002. The Influence of Damper Properties on Vehicle Dynamic Behaviour. SAE Technical Paper 2002-01-0319. Society of Automotive Engineers. http://dx.doi.org/10.4271/2002-01-0319.

Sun, Y., Zhang, M., Zhao, F., 2011. Reflective cracking dynamic response of asphalt concrete under vehicle loading. In: 2011 Second International Conference on Mechanic Automation and Control Engineering, Hohhot, 2011.

Zhang, Y., Zhang, X., 2011. Dynamic response analysis of pavement and subgrade of highway. In: 2011 International Conference on Multimedia Technology, Hangzhou, 2011.

Zhu, S.P., Huang, H.Z., Wang, Z.L., 2011. Fatigue life estimation considering damaging and strengthening of low amplitude loads under different load sequences using fuzzy sets approach. International Journal of Damage Mechanics 20 (6), 876–899. http://dx.doi.org/10.1177/1056789510397077.